

Supplemental Information

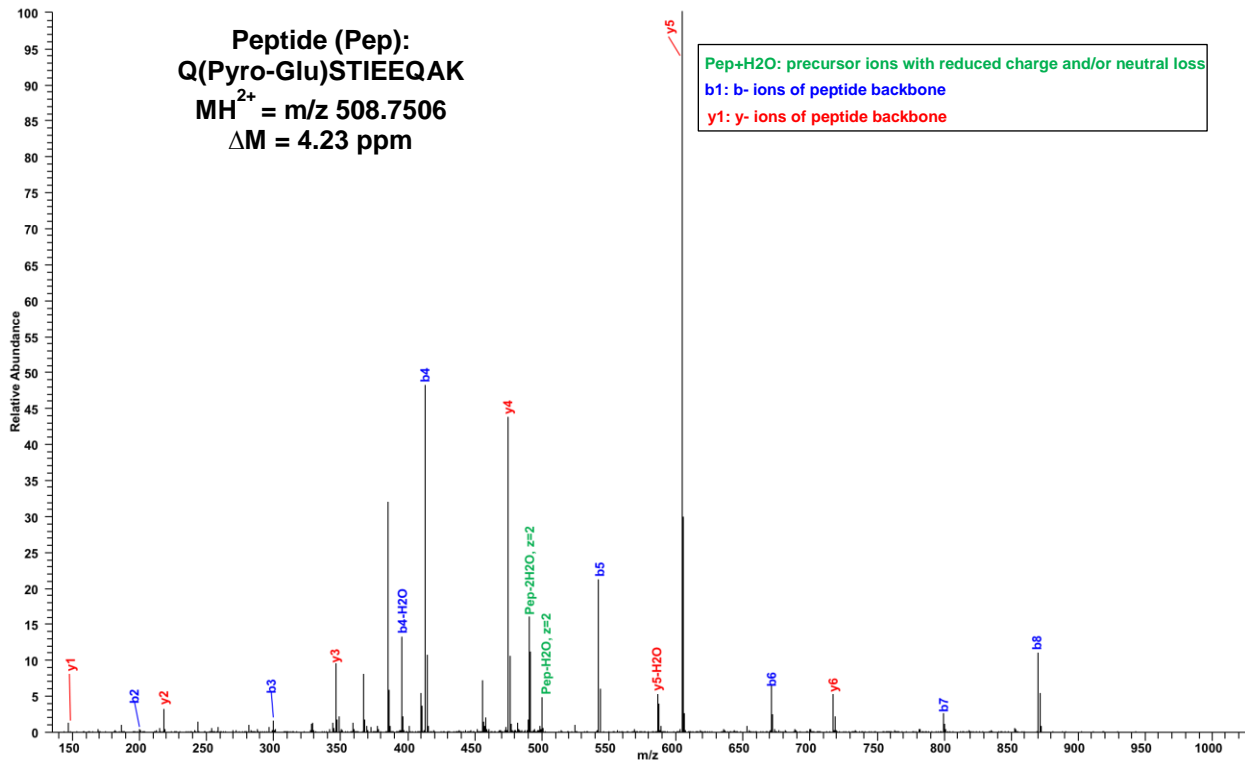
**Virus-Receptor Interactions of Glycosylated
SARS-CoV-2 Spike and Human ACE2 Receptor**

Peng Zhao, Jeremy L. Praissman, Oliver C. Grant, Yongfei Cai, Tianshu Xiao, Katelyn E. Rosenbalm, Kazuhiro Aoki, Benjamin P. Kellman, Robert Bridger, Dan H. Barouch, Melinda A. Brindley, Nathan E. Lewis, Michael Tiemeyer, Bing Chen, Robert J. Woods, and Lance Wells

Supplemental Information

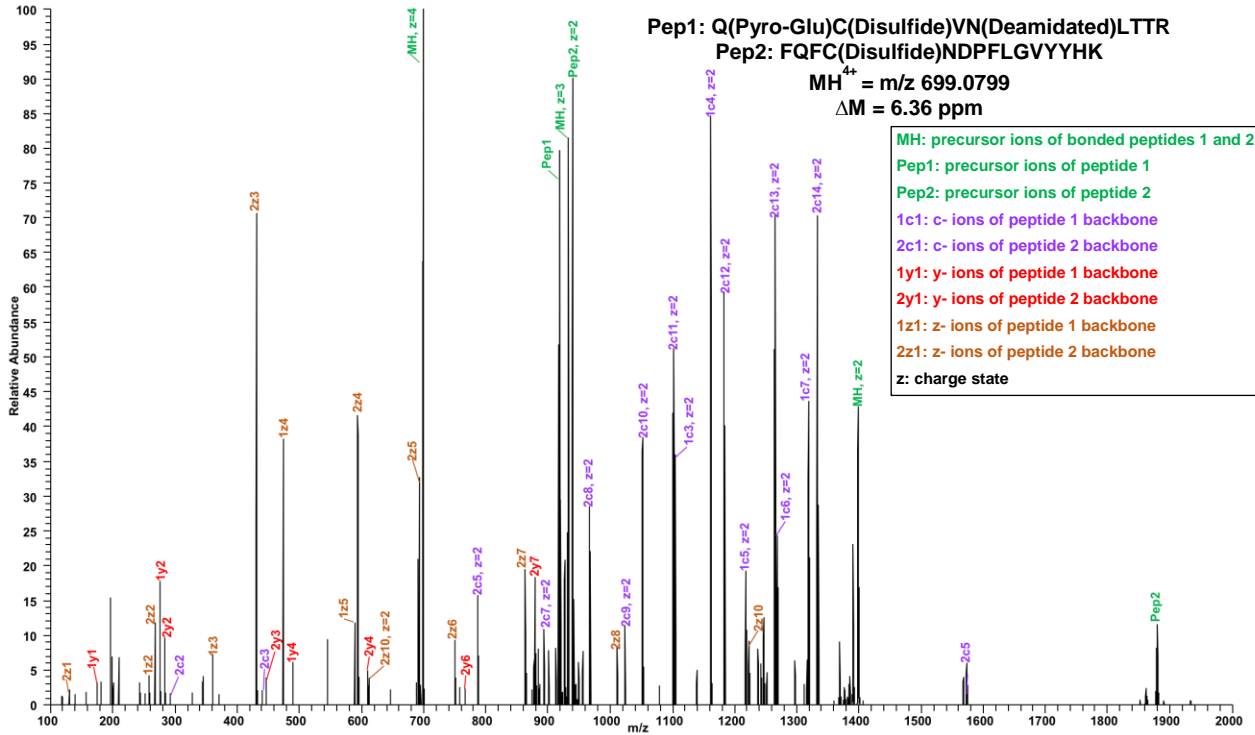
**Virus-Receptor Interactions of Glycosylated
SARS-CoV-2 Spike and Human ACE2 Receptor**

Peng Zhao, Jeremy L. Praissman, Oliver C. Grant, Yongfei Cai, Tianshu Xiao, Katelyn E. Rosenbalm, Kazuhiro Aoki, Benjamin P. Kellman, Robert Bridger, Dan H. Barouch, Melinda A. Brindley, Nathan E. Lewis, Michael Tiemeyer, Bing Chen, Robert J. Woods, and Lance Wells



Supplemental Figure S1. Defining N-terminus of ACE2 as pyro-glutamine at site Q0018.

Related to Figure 1. Representative HCD MS2 spectrum shown.



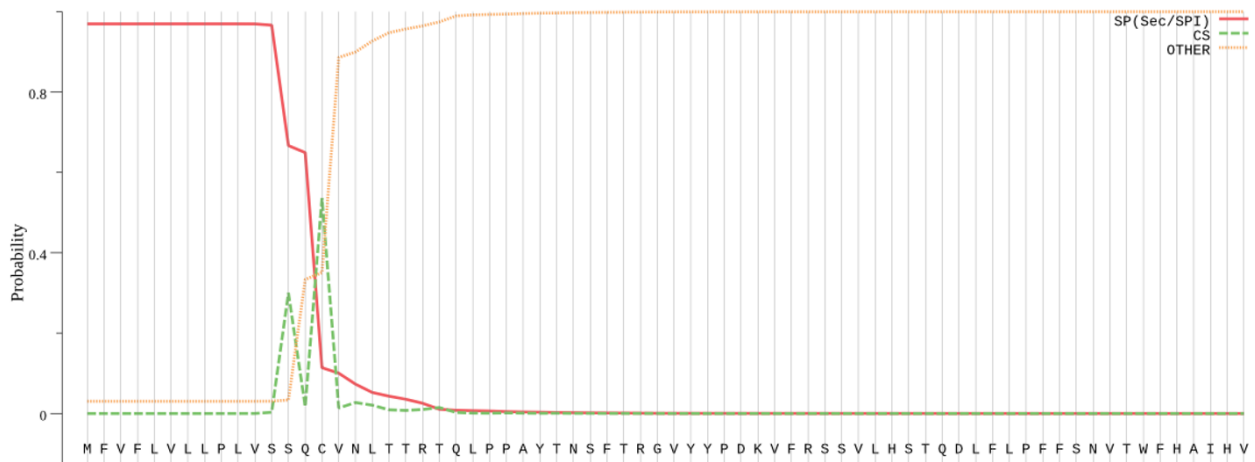
Supplemental Figure S2. Disulfide bond formed between Cysteines 0015 and 0136 of SARS-CoV-2 S.

Related to Figure 1. Representative EThcD MS2 spectrum shown.

Utilized Start Met: MFVFLVLLPLVSSQCVNL...

Signal P: SSQC-VN (.54)

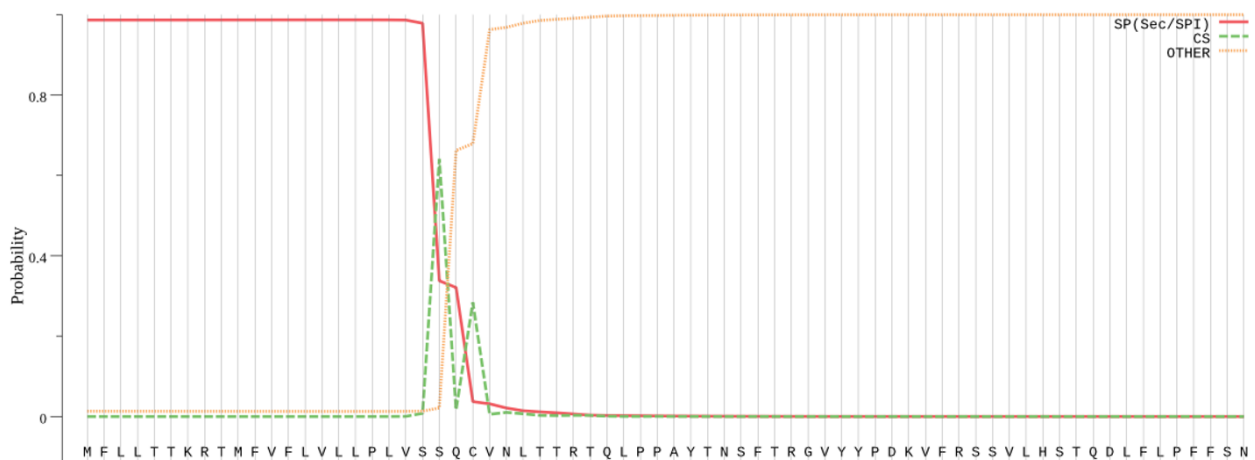
SignalP-5.0 prediction (Eukarya): Sequence



Upstream Met: MFLLTTKRTMFVFLVLLPLVSSQCVNL...

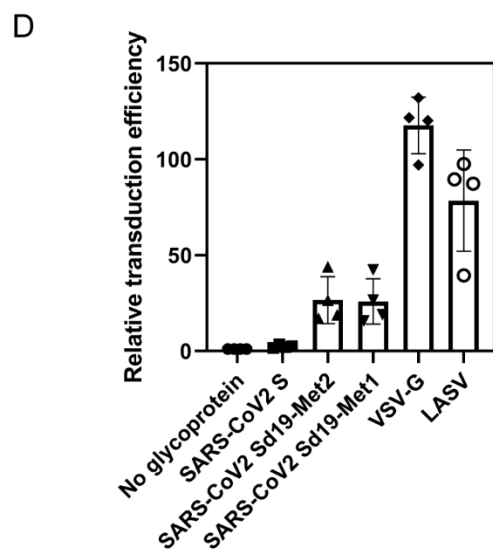
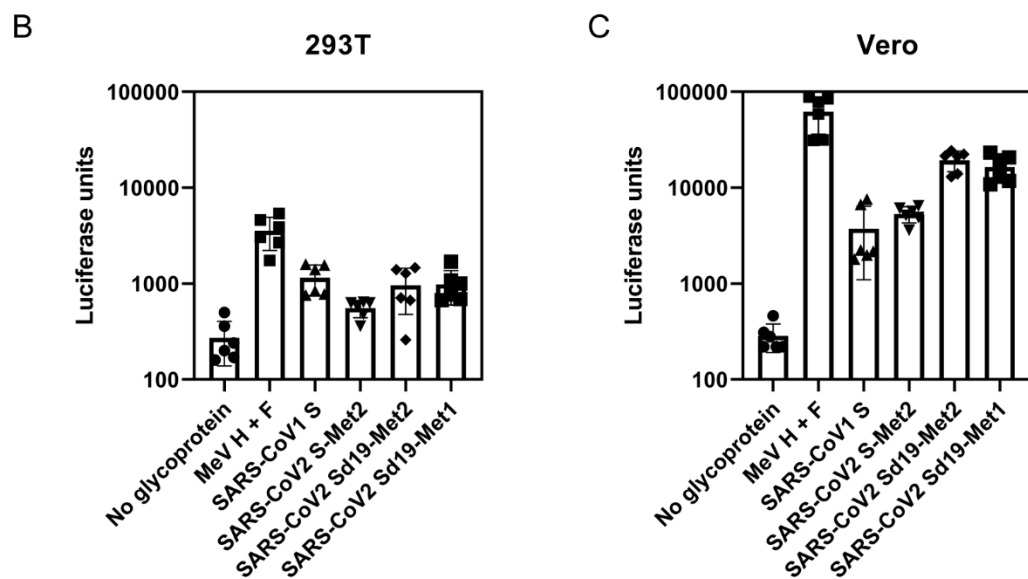
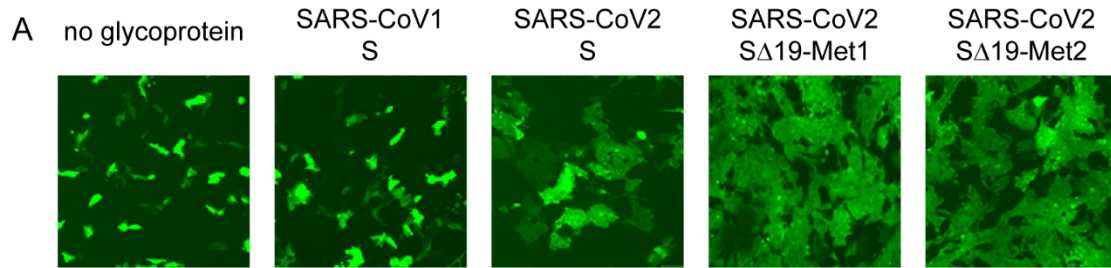
Signal P: SS-QCVN (.64)

SignalP-5.0 prediction (Eukarya): Sequence



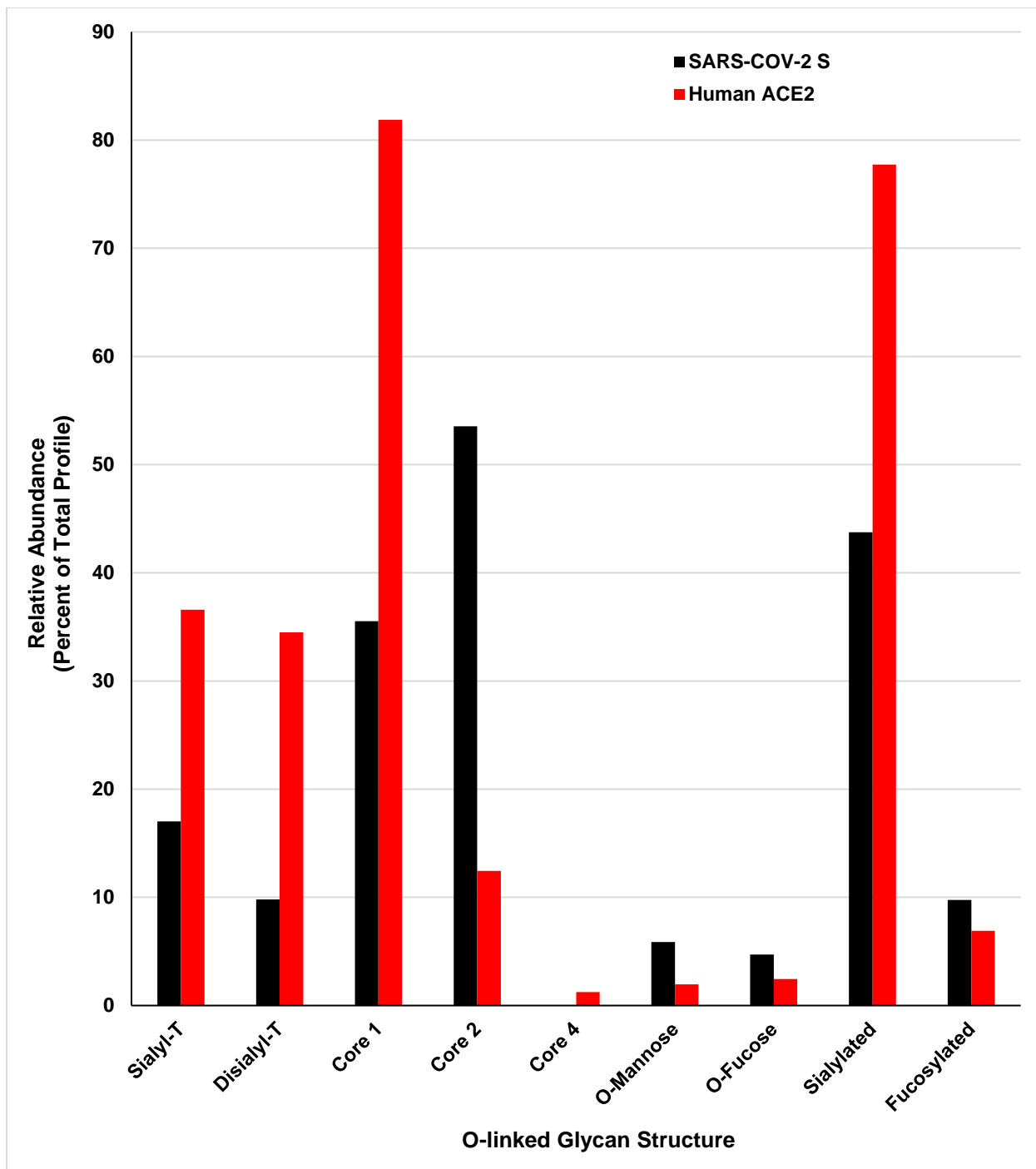
Supplemental Figure S3. Signal P prediction of two different start methionines for SARS-CoV-2 S.

Related to Figure 1.



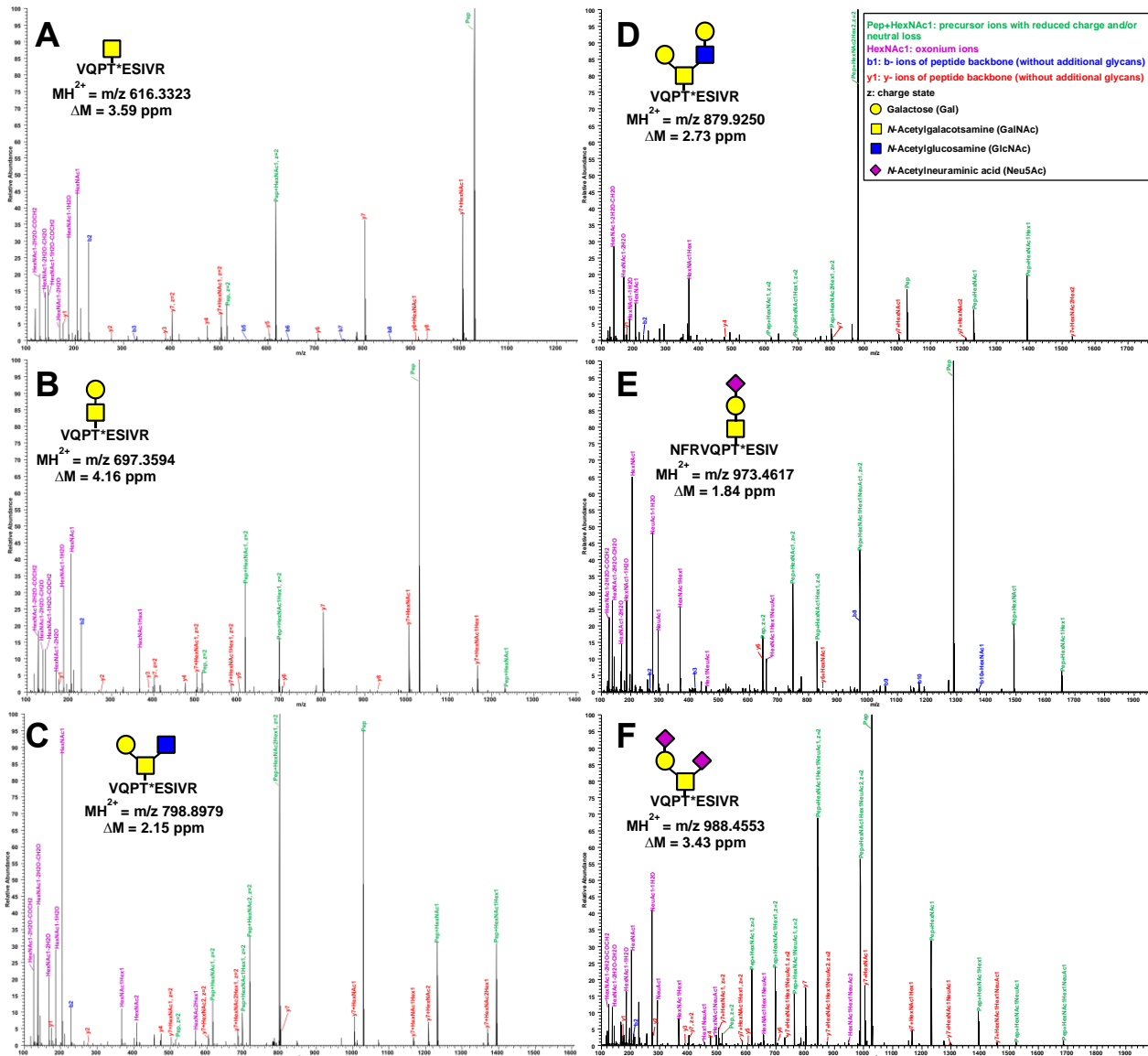
Supplemental Figure S4. Functional characterization of various S constructs in Pseudovirus.

Related to Figure 1. **(A)** Syncytia produced by SARS-CoV-2 S constructs in VeroE6 cells co-transfected with a GFP plasmid to visualize cell-to-cell fusion. Quantification of fusion using a luciferase complementation assay in 293T **(B)** or VeroE6 cells **(C)**. **(D)** Transduction efficiency in Vero E6 cells of ppVSV-GFP particles coated in the indicated glycoprotein. Results suggest that start methionine does not alter fusion or efficiency.



Supplemental Figure S5. Detection of O-linked glycans released from SARS-CoV-2 S and human ACE2.

Related to Figure 4. The detected O-glycans were categorized based on their structures and types. Relative abundance (prevalence) of each species is calculated based on peak intensity in full MS.



Supplemental Figure S6. O-linked glycans detected at site T0323 of SARS-CoV-2 S.

Related to Figure 4. Representative Step-HCD spectra shown for 6 glycoforms.

A

CoV-1R MFIFLLFLTLTSGSDLRCCTTFDQVAP **WY** QHTSSMRGVYYPPDEIFRSSTDLYTQLDFL
 CoV-2I MFVFLVPLPVS-**QCNCVLT**TRTQL-PPAYT-NSFTRVYYPDKVFRSLVHSQDFL
 .;*.*;*.*;*.*;*.*;*.*;*.*;*.*;*.*;*.*;*.*;*.*;*.*;*.*;*.*;*.*;
VAR1
 CoV-1R PEYVSNTGFGHTI-----**WT**-FGNPV1PFKDGTYYFAATEKSNVWRGVWFGSTMN**KQS**
 CoV-2I PEFSWVNFHAIHVSGTGK1KFDPNVLPFNDGVYEASTEKSNIIRGWFITGLDSKTQ5
 .;*.*;*.*;*.*;*.*;*.*;*.*;*.*;*.*;*.*;*.*;*.*;*.*;*.*;*.*;
VAR2
 CoV-1R VILIINNSNVVIRCAFNCLFDNNFFAV---SKPMGTOHTMIDFNAFICATVYEFSDAIS
 CoV-2I LLINNAVVIKVCVEQFCNDFPLGLYVHHNN**KQS**MSEEFREVYSSANCFEVYSSOPFL
 .;*.*;*.*;*.*;*.*;*.*;*.*;*.*;*.*;*.*;*.*;*.*;*.*;*.*;*.*;
VAR3
 CoV-1R LDVEKSGNFKLHREFVFKNKGDFLYVVKYQPIDVVRDLPSGFNTLKPIFKLPLGI**NIT**
 CoV-2I MDLGEKGQNFKNLREFVFKNKGDFYK1SCHKTPN1RLPDGFSALEPVLPIG1**NIT**
 .;*.*;*.*;*.*;*.*;*.*;*.*;*.*;*.*;*.*;*.*;*.*;*.*;*.*;*.*;*.*;
VAR4
 CoV-1R NFRAIL-----TAFSPQAQT - WGTSAAAYFVGVLKPPTFLMKYDE **NG**1TIDAVDCDSNQLP
 CoV-2I RFTQLLAHLRSYLTPGDSSGWTAGAAAYYGGYLOPRTFLKYN **NG**1TIDAVDCALDPL
 .;*.*;*.*;*.*;*.*;*.*;*.*;*.*;*.*;*.*;*.*;*.*;*.*;*.*;*.*;*.*;
VAR5
 CoV-1R AELKCSVKSFEIDQYIQTSMNRVPSGVDFRPNTNLCPGEVFTAKFPSVVAWER
 CoV-2I SETKTCLSFTVEKGVIQTSFMRVPTES1VPRFLN1LCPGEVFTAKFASVYAWNRK
 .;*.*;*.*;*.*;*.*;*.*;*.*;*.*;*.*;*.*;*.*;*.*;*.*;*.*;*.*;
CoV-1R KISCNVADSVLY**NS1** FFSTFKCYGVSATKLNDLCFSNWYADSFVKGDDVRQIAQPGQT
CoV-2I RTISCNVADSVLYNSAFSTFKCYGVSPFLKNDLNFNTVNADSVFVR1GEVDQRAQPGQT
 .;*.*;*.*;*.*;*.*;*.*;*.*;*.*;*.*;*.*;*.*;*.*;*.*;*.*;*.*;*.*;
CoV-1R VIADYNYKL PDDFMGCVLAWNTRN1DA STGHNYYNQYRLHGKLRLPFRDISNVPSPD
CoV-2I KIADYNYKL PDDFTCGVIAWNSNLDLSKVGNNYNYLRLFRKSNLKPFERDISTIEVQAG
 .;*.*;*.*;*.*;*.*;*.*;*.*;*.*;*.*;*.*;*.*;*.*;*.*;*.*;*.*;*.*;
CoV-1R GKPCPT-PALCNYPLNLDYQVTTGIGQYPRVRLSFELLNAPATVCPGKLSTDILK
CoV-2I STPCNGVFGNCYFCPLQSQYFQPTNGQYVPRVWLSEFLLLHAPATVCPGKKSTNLVKN
 .;*.*;*.*;*.*;*.*;*.*;*.*;*.*;*.*;*.*;*.*;*.*;*.*;*.*;*.*;*.*;
CoV-1R QCWNFNGFLTGTGVLTPSKRFQPFQGGRDVSFDTSVDRPKTEI1LDISPCAFGWS
CoV-2I KCVNFGFLTGTGVLTESENKCFPQGQFRDIADTADVRPQTEI1LDISPCAFGWS
 .;*.*;*.*;*.*;*.*;*.*;*.*;*.*;*.*;*.*;*.*;*.*;*.*;*.*;*.*;*.*;
CoV-1R VITPGT**NS1**SEAVLVYQDV**NC1**DVSTAIHADQLTPAWRIYSTGNNWFQ7QAGCLIGAEHV
CoV-2I VITPGT**NS1**NOAVLVYQDV**NC1**EVPWAH1DAOLTPTRWVRYSTGSNFQ7TRAGCLIGAEHV
 .;*.*;*.*;*.*;*.*;*.*;*.*;*.*;*.*;*.*;*.*;*.*;*.*;*.*;*.*;*.*;
VAR4
CoV-1R DTSYECIDIPIGACIASYHTVSL-----R 667
CoV-2I **NS1**SYECIDIPIGACIASYQTSPNGSG 685
 .;*.*;*.*;*.*;*.*;*.*;*.*;*.*;*.*;*.*;*.*;*.*;*.*;*.*;*.*;*.*;

B

Supplemental Figure S7. Sequence alignments of SARS-CoV-1 and SARS-CoV-2 S variants as well as alignment of multiple S proteins from related coronaviruses.

Related to Figure 4.